Free vibration of CLT plates

Jussi-Pekka Matilainen[1] and Jari Puttonen

Summary. This article discusses the ability of different methods to predict the natural frequencies of vibration for a cross laminated timber (CLT) plate. The prediction models considered are the method proposed by Finnish design code for timber structures (RIL), the classical laminated plate theory (CLPT), the first-order shear deformation theory (FSDT) and the finite element method with a shell element (S4R) of Abaqus code. The basic principles governing the dynamic behavior of an orthotropic plate are explained and the effect of shear deformation on the predicted frequencies is illustrated. Constitutive equations for a CLT plate are shown and their implication on the mode shapes is explained. Suitability of the prediction models to the CLT plates are evaluated by comparing them with two different laboratory experiments. First, an experiment carried out by Maldonado & Chui (2012) is illustrated in order to highlight the effect of aspect ratio on natural frequencies. Finally, results of a new experiment conducted for this study demonstrate the effect of side-to-thickness ratio on measured and predicted frequencies.

Introduction

CLT is a massive timber product, which is used in load bearing applications such as plates and shear walls. CLT elements are made up of ordinary boards, glued together in a cross-layered fashion and typically showing symmetric layup (Stürzenbecher, et al., 2010). Since timber is a relatively soft and lightweight construction material, the design of such structures is driven by serviceability criteria like maximum deflections and vibration susceptibility (Gsell, et al., 2007). The serviceability of timber floors becomes more and more relevant due to the use of high strength materials and longer spans (Hamm, et al., 2010). Floor vibration is taken into account in the European design code for timber structures, in which it is required that the fundamental frequency of a timber floor should be assessed (CEN, 2004). However, the dynamic behavior of CLT floor systems differs from that of traditional lightweight wood-joisted floors and heavy concrete slabs. Therefore the existing design codes may not be able to predict the fundamental frequencies accurately (Hu & Gagnon, 2012). The purpose of this article is to describe the dynamic behavior of a CLT plate and to assess suitable methods for evaluating the natural frequencies of a CLT floor.

[1]Corresponding author. jussi-pekka.matilainen@outlook.com

Dynamic behavior of a CLT plate

In order to gain a basic understanding of the dynamic behavior of a CLT plate, a brief review of mechanics of laminated composite plates is required. Reddy (2003) provides a comprehensive treatment on the subject.

The simplest laminated plate theory is the classical laminated plate theory (CLPT), which is an extension of the Kirchhoff plate theory to laminated composite plates. Assumptions of the Kirchhoff plate theory neglect both the transverse shear and normal stresses. Therefore, the plate deformation is entirely due to bending and in-plane stretching which implies that the Kirchhoff assumptions are valid only for relatively thin plates. Practical consequences of the Kirchhoff assumptions lead to overprediction of the natural frequencies with relatively thick plates because the shear deformations are not accounted for.

Relaxation of the Kirchhoff assumptions by including a constant state of transverse shear stresses through the laminate thickness results in the first-order shear deformation theory (FSDT). FSDT is based on the Mindlin plate theory, which assumes a linear variation of displacements across the plate thickness while maintaining the transverse inextensibility of the plate thickness. Since the FSDT takes into account shear deformation, it is recommended to be used with relatively thick plates. However, the assumption of constant state of transverse shear stresses violates the boundary conditions at the plate surfaces where shear stresses should vanish. Therefore, the FSDT requires shear correction factors to correct the unrealistic variation of the shear stresses through the thickness. A well-known value for the shear correction factor for homogeneous plates is $K = 5/6$, but this value is different for every laminated plate. In order to avoid the use of shear correction factors, higher-order shear deformation theories (HSDT) have been developed. They involve higher-order stress resultants that are difficult to interpret physically and are not dealt with in this article.

From the mechanical point of view, CLT plate is a symmetric cross-ply laminated plate in which the ply stacking sequence, material properties and geometry are symmetric about the mid-plane. Because of this symmetry, coupling is eliminated between extension and shear as well as between bending and twisting. Therefore, the symmetric laminates have no tendency for twisting, and both the force and moment resultants for a symmetric laminate have the same form as the orthotropic single-layer plates. The constitutive equations for a symmetric cross-ply laminate based on the classical and first-order theories are given by:

$$
\begin{Bmatrix} N_{xx} \\ N_{yy} \\ N_{xy} \end{Bmatrix} = \begin{bmatrix} A_{11} & A_{12} & 0 \\ A_{12} & A_{22} & 0 \\ 0 & 0 & A_{66} \end{bmatrix} \begin{Bmatrix} \varepsilon_{xx}^0 \\ \varepsilon_{yy}^0 \\ \gamma_{xy}^0 \end{Bmatrix},
\tag{1}
$$

$$
\begin{Bmatrix} M_{xx} \\ M_{yy} \\ M_{xy} \end{Bmatrix} = \begin{bmatrix} D_{11} & D_{12} & 0 \\ D_{12} & D_{22} & 0 \\ 0 & 0 & D_{66} \end{bmatrix} \begin{Bmatrix} \kappa_{xx} \\ \kappa_{yy} \\ \kappa_{xy} \end{Bmatrix},
\tag{2}
$$

$$
\begin{Bmatrix} Q_y \\ Q_x \end{Bmatrix} = K \begin{bmatrix} A_{44} & 0 \\ 0 & A_{55} \end{bmatrix} \begin{Bmatrix} \gamma_{xy}^0 \\ \gamma_{xz}^0 \end{Bmatrix},
\tag{3}
$$

where the in-plane force resultants are denoted as N_{xx}, N_{yy} and N_{xy}, the moment resultants as M_{xx}, M_{yy} and M_{xy} and the transverse force resultants as Q_x and Q_y. The mid-plane strains of the laminate are expressed as ε_{xx}^0, ε_{yy}^0, γ_{xy}^0 and γ_{xz}^0 while the curvatures are expressed as κ_{xx}, κ_{yy} and κ_{xy}. The extensional and bending stiffnesses are given by A_{ij} and D_{ij}, respectively, while the shear correction coefficient is given by K.

From the Equations 1 to 3, it can be seen that the coupling between normal forces and shearing strain and normal moments and twist is zero (i.e. A_{16}, A_{26}, D_{16} and D_{26} are zero). In terms of dynamic behavior, this implies that the mode shapes of a CLT plate remain aligned with the laminate axes. However, in case of generally orthotropic layers (i.e., the principal material coordinates do not coincide with those of the plate) the mode shapes tend to twist. The principal material coordinates refer to the directions parallel and perpendicular to the fibres in an orthotropic layer. Example of this is provided by Figure 1, where the second mode shapes of a specially orthotropic plate and an angle-ply plate with 45° rotation to the plate coordinate system are compared.
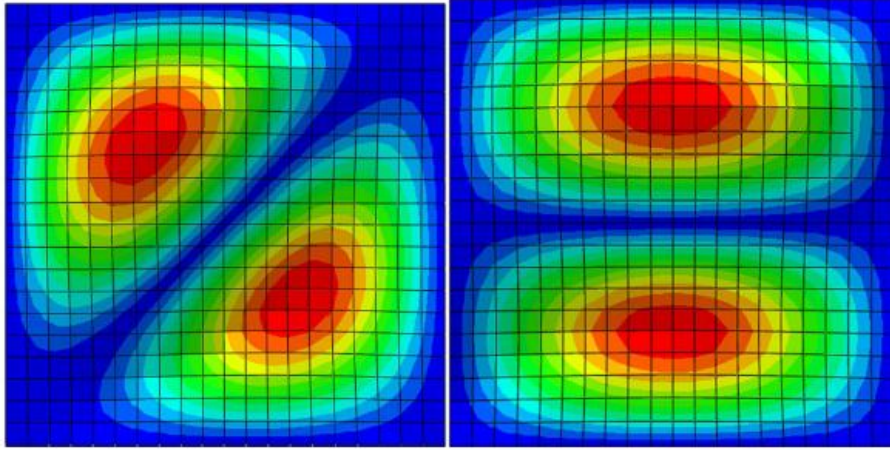
Figure 1. Mode shapes of an angle-ply (left) and specially orthotropic plates (right).

It is of interest to study the dynamic behavior predicted by the CLPT and FSDT of a specially orthotropic plate through the Navier problem where a rectangular plate is simply supported on all four edges. The natural frequency of a specially orthotropic single-layer plate depends on many parameters such as plate aspect ratio (a/b), modulus ratio (E_1/E_2) and side-to-thickness ratio (a/h). In this context, a and b denote the in-plane dimensions along the x- and y-coordinate directions of the rectangular laminate while E_1 and E_2 denote the moduli of elasticity in these directions, respectively. The geometry and coordinate system for a simply supported rectangular plate are shown in Figure 2.

Natural frequencies of an orthotropic plate can be solved as eigenvalues of well-known free vibration problem

$$det([K] - \omega^2[M]) = 0, \tag{4}$$

where $[K]$ is the stiffness matrix, $[M]$ is the mass matrix and ω is the circular frequency of vibration.
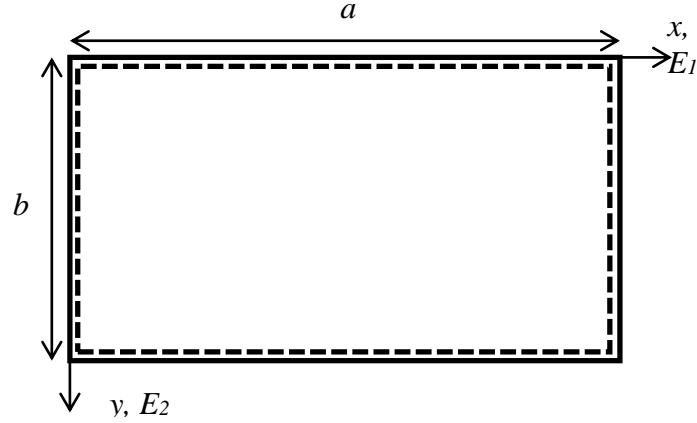
Figure 2. Geometry and coordinate system for a simply supported rectangular plate.

CLPT solution of Equation (4) in terms of cyclic frequencies is given by (Reddy, 2003):

$$f_{m,n} = \frac{\pi}{2a^2} \sqrt{\frac{D_{11}}{\rho h}} \sqrt{m^4 + \left[2\frac{D_{12} + 2D_{66}}{D_{22}}m^2n^2\left(\frac{a}{b}\right)^2 + \left(\frac{a}{b}\right)^4 n^4\right]\frac{D_{22}}{D_{11}}}, \qquad (5)$$

where f is the cyclic frequency, ρ is the density, h is the plate thickness and a and b denote the planar dimensions of the plate. The cyclic frequency f is related to the circular frequency by $f = \omega/2\pi$.

For different values of m and n, there is a unique frequency $f_{m,n}$ and a corresponding mode shape. For plates supported on four sides, m and n define the number of half sine waves in the a and b directions, respectively. The corresponding FSDT solution in terms of circular frequencies can be found in the work of Reddy (2003) but, for brevity, is not presented in this article.

In order to assess the applicability of current design practice to the prediction of natural frequencies of CLT plates, a model used in Finland is taken into consideration. For a rectangular floor which is simply supported along all four edges, the Finnish Association of Civil Engineers (RIL, 2009) suggests that the fundamental frequency may approximately be calculated as

$$f_1 = \frac{\pi}{2l^2} \sqrt{\frac{(EI)_l}{\rho h}} \sqrt{1 + \left[2\left(\frac{l}{B}\right)^2 + \left(\frac{l}{B}\right)^4\right]\frac{(EI)_B}{(EI)_l}}, \qquad (6)$$

where the floor spans are given by $l = a$ and $B = b$ while the plate bending stiffnesses of the floor about an axis are given by $(EI)_l, (EI)_B = D_{11}, D_{22}$.

It can be shown that the Equation (6) is derived from the CLPT, Equation (5), with an assumption that the Poisson's ratio is assumed constant.

For comparison, the fundamental frequencies are also calculated with Abaqus/Standard which is a finite element analysis program. The plate is modeled with general-purpose conventional shell element S4R which allows transverse shear deformation. S4R stands for a 4-node, quadrilateral, shell element with reduced integration. (Abaqus, 2012)

For convenience, the following nondimensional fundamental circular frequency is used in presenting the numerical results in graphical forms in this article:

$$\bar{\omega} = \omega \frac{b^2}{\pi^2} \sqrt{\frac{\rho h}{D_{22}}}, \tag{7}$$

Figure 3 shows a plot of nondimensionalized fundamental circular frequency $\bar{\omega}$ as a function of plate aspect ratio a/b, Figure 4 shows a plot of $\bar{\omega}$ as a function of modulus ratio E_1/E_2 and Figure 5 shows a plot of $\bar{\omega}$ as a function of side-to-thickness ratio a/h. The following material properties are used to represent typical values for a CLT plate made of spruce:

$$E_1/E_2 = 30, G_{12} = G_{13} = 1.9E_2, v_{12} = 0.44, \tag{8}$$

From Figure 3 it can be seen that all the models used (RIL, CLPT, S4R) behave in the same manner as function of aspect ratio a/b. Clearly, the fundamental frequency increases as the stiffer side (a) becomes relatively shorter than the softer side (b). Figure 4 demonstrates that the fundamental frequency increases with modular ratio E_1/E_2 with all the models used (RIL, CLPT, S4R). Figure 5 reveals the main differences between the models. Two models (RIL and CLPT) are totally insensitive to side-to-thickness ratio a/h and the only difference between these models is due to the approximation adopted in the RIL model. Instead, the shear deformation models (S4R and FSDT) demonstrate that the fundamental frequency begins to decrease with lower values of a/h as the shear deformation steps into the picture.
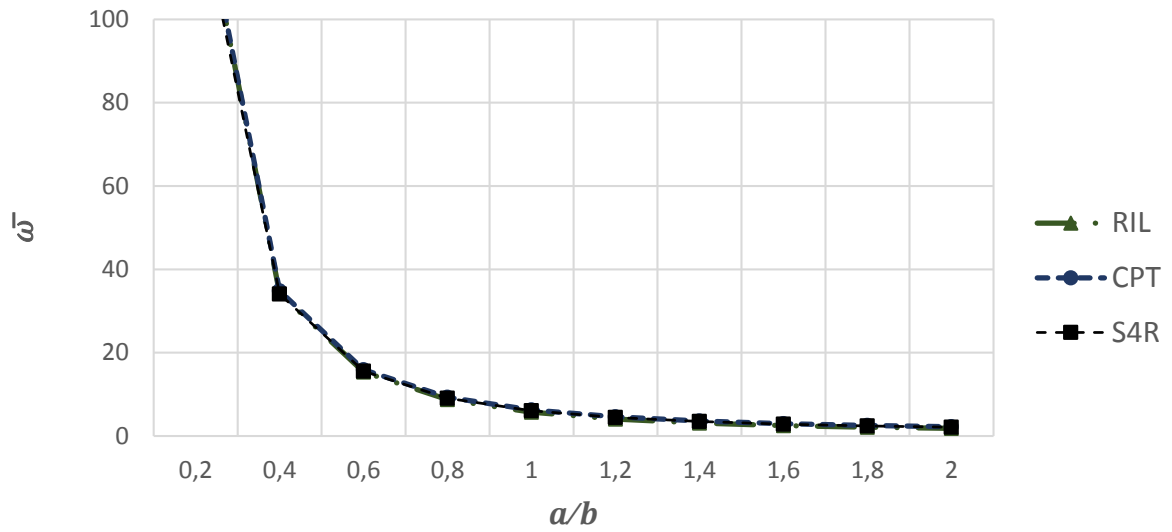
Figure 3. Nondimensionalized fundamental frequency ($\bar{\omega}$) as a function of plate aspect ratio (a/b) for simply supported, orthotropic and single-layer plate.
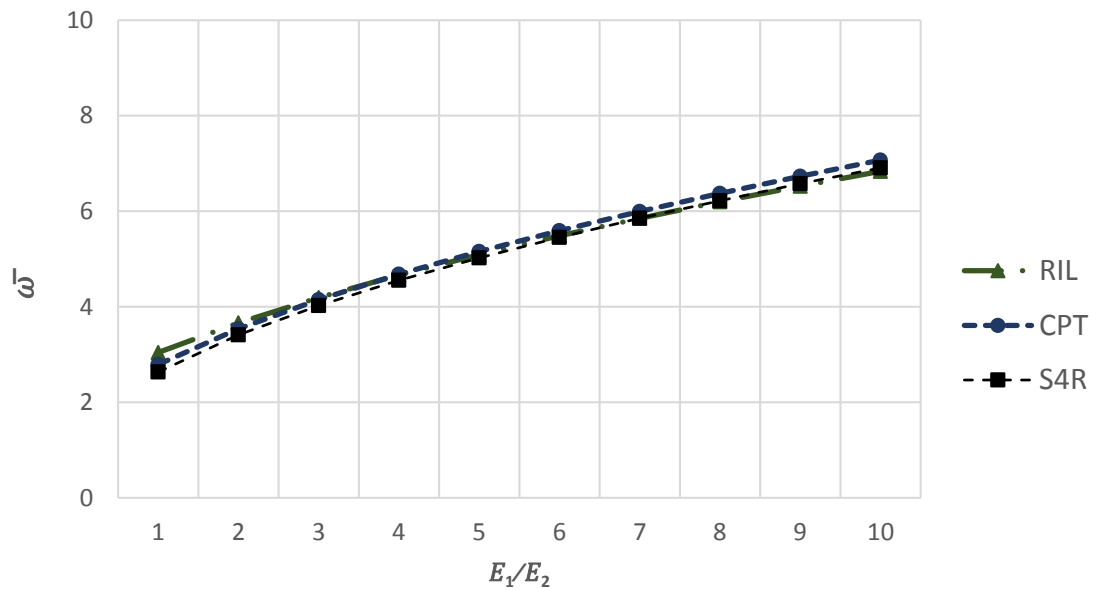
Figure 4. Nondimensionalized fundamental frequency ($\bar{\omega}$) as a function of modulus ratio (E_1/E_2) for simply supported, orthotropic and single-layer plate.
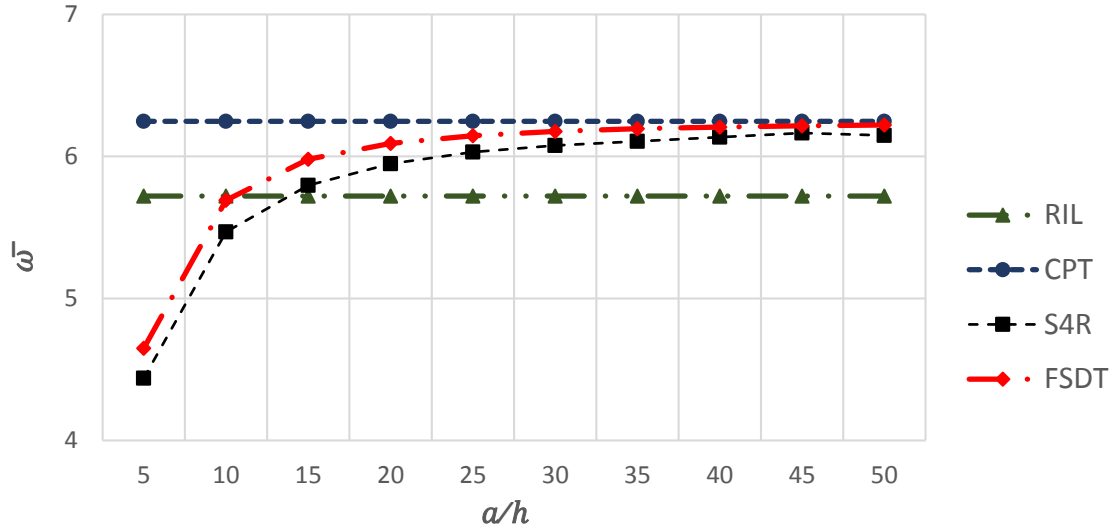
Figure 5. Nondimensionalized fundamental frequency ($\overline{\omega}$) versus side-to-thickness ratio (a/h) for simply supported, orthotropic and single-layer plate.

Experimental vibration tests

CLT floor tests by Maldonado & Chui (2012)

In order to assess the suitability of the presented methods to predict natural frequencies of a CLT plate, experimental results are evaluated for comparison. Maldonado & Chui (2012) performed vibration tests for a 5 layer CLT panels with the following dimensions: 1.020 m x 4.870 m x 0.132 m. A total of four CLT panels were used to construct a 4.870 m x 4.080 m CLT floor in the laboratory. A test where the floor was supported on all four sides was conducted. The floor width was progressively increased by adding a second, third and a final fourth panel to the floor specimen. The floor was retested at each floor width. The adjacent panels were connected by self-tapping screws with 30 cm spacing. Connection of the adjacent panels is shown in Figure 6. Density of the CLT panel was measured to 560 kg/m^3 while the elastic properties equivalent to a single-layer plate were evaluated to be E_1=11700 MPa and $E_2 = 9000$ MPa based on the vibration test. In order to model the mechanical properties of the panel accurately, the following mechanical properties are assumed in this article: layers in the longitudinal and transverse directions are of strength classes C24 and C18 according to RIL (2009), respectively. The assumed mechanical properties are shown in Table 1. In addition, a shear correction factor of $K = 0.6$ was assumed for the laminated plate.

Three different modes of natural vibration ($f_{1,1}, f_{2,1}, f_{3,1}$) were identified with four different aspect ratios a/b. The notation $f_{m,n}$ defines the frequency f with mode shape (m, n). For plates supported on four sides, m and n define the number of half sine waves in the a and b directions, respectively. Experimental values for the natural frequencies from Maldonado & Chui (2012) and results from different prediction methods are shown

23

in Table 2. The corresponding mode shapes are shown in Figure 7. Since the floor width b was the only variable in this experimental setup it is interesting to study how the measured natural frequencies developed as a function of aspect ratio (a/b) compared to the predicted values. The effect of aspect ratio on the nondimensionalized frequencies $\overline{\omega}_{1,1}$, $\overline{\omega}_{2,1}$ and $\overline{\omega}_{3,1}$ for the experimental as well as predicted values is shown in Figures 8, 9 and 10, respectively.

From the Figures 8, 9 and 10 it is seen that the experimental results behave according to the theoretical curves shown in Figure 1. This is natural since in this experiment the natural frequency is noted to decrease as the floor width is increased. In addition, the shear deformation models FSDT and S4R seem to follow the experimental curve quite well for every value of a/b whereas the models RIL and CLPT seem to overestimate the natural frequencies. This is attributed to the increase of relative thickness and, consequently, to the effect of shear deformation. It is also noted that the most distinctive discrepancy between the experimental and predicted results occurs at the fundamental frequency $\overline{\omega}_{1,1}$. In this case the floor specimen clearly behaves in a more flexible manner in comparison with the prediction models. This is assumed to be caused by the connection configuration shown in Figure 6 which seems to prevent the floor specimen to act in a completely monolithic way during the first mode of vibration. For higher frequencies the prediction models become more accurate as the multiple half-sine waves acting upon the floor enhance interlocking between the panels.

Although the exact material properties of the CLT plate used in the experimental setup are not known exactly and the material properties used in the models are assumed, the accuracy of the prediction models is evaluated on the basis of relative difference with the experimental results. Table 3 shows the relative difference for a certain mode of natural vibration and the mean error of a prediction model.

From Table 3 it is noted that the predicted fundamental frequency $f_{1,1}$ deviates more from the experimental result for every model. The shear deformation models FSDT and S4R predict clearly more accurate results overall than the model based on the Kirchhoff assumption (RIL and CLPT). Considering the initial uncertainty in the material parameters, the overall accuracy of the shear deformation models with approximately 10 % difference with the experimental results seems acceptable. On the other hand, the code based model (RIL) produces an error of about 30 % and therefore it is questionable if the model is suitable to predict the natural frequencies of a CLT floor.

Table 1. Mechanical properties of the CLT panel with strength classes C24 and C18 (RIL, 2009).

Layer	Thickness (mm)	E_1 (MPa)	E_2 (MPa)	v_{12}	G_{12} (MPa)	G_{13} (MPa)	G_{23} (MPa)
1	26.4	11000	370	0.44	690	690	50
2	26.4	300	9000	0.015	560	50	560
3	26.4	11000	370	0.44	690	690	50
4	26.4	300	9000	0.015	560	50	560
5	26.4	11000	370	0.44	690	690	50
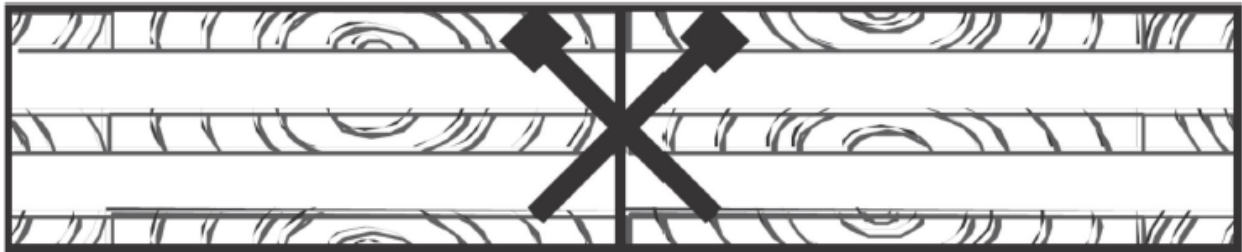
Figure 6. CLT panel connection configuration during the experiment. (Maldonado & Chui, 2012)
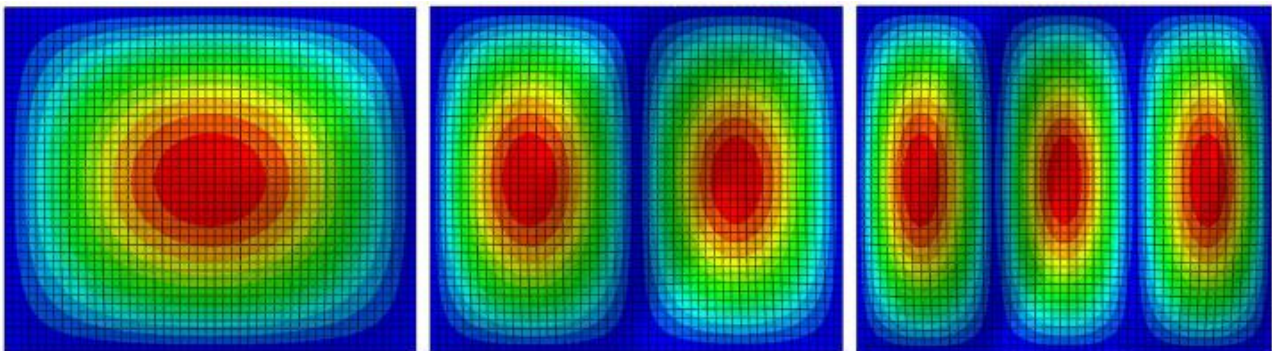
Figure 7. Mode shapes of frequencies $f_{1,1}$, $f_{2,1}$ and $f_{3,1}$ of CLT floor (four panels) supported on four sides.

Table 2. Experimental values from Maldonado & Chui (2012) and results from different prediction method

$\dfrac{a}{b}$	$f_{1,1}$ (Hz)	$f_{2,1}$ (Hz)	$f_{3,1}$ (Hz)	Results	
4.8	79	102.75	126		
2.4	22	47.25	79.25		Maldonado& Chui (2012)
1.6	15.75	42	76.25		
1.2	12	39.5	74		
4.8	118.8	137.9	176.6		
2.4	34.5	59.5	107.2		RIL 205-1- 2009
1.6	19.6	47.6	97.1		
1.2	14.9	44.0	93.9		
4.8	117.3	132.5	167.2		
2.4	33.1	56.4	103.3		CLPT
1.6	18.6	45.9	95.2		
1.2	14.1	43.0	92.8		
4.8	83.3	97.3	129.2		
2.4	29.9	52.2	94.8		FSDT
1.6	17.8	44.1	89.0		
1.2	13.8	41.6	87.2		
4.8	91.9	101.1	121.4		
2.4	30.7	49.3	82.3		S4R
1.6	17.5	40.7	76.3		
1.2	13.4	38.3	74.6		
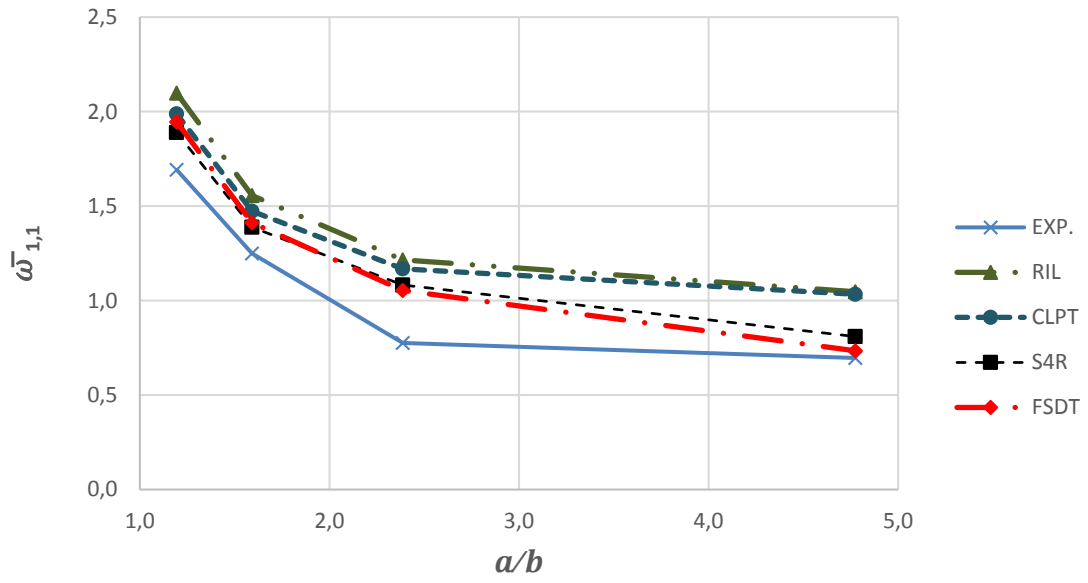
Figure 8. The effect of aspect ratio on nondimensionalized frequencies $\bar{\omega}_{1,1}$.
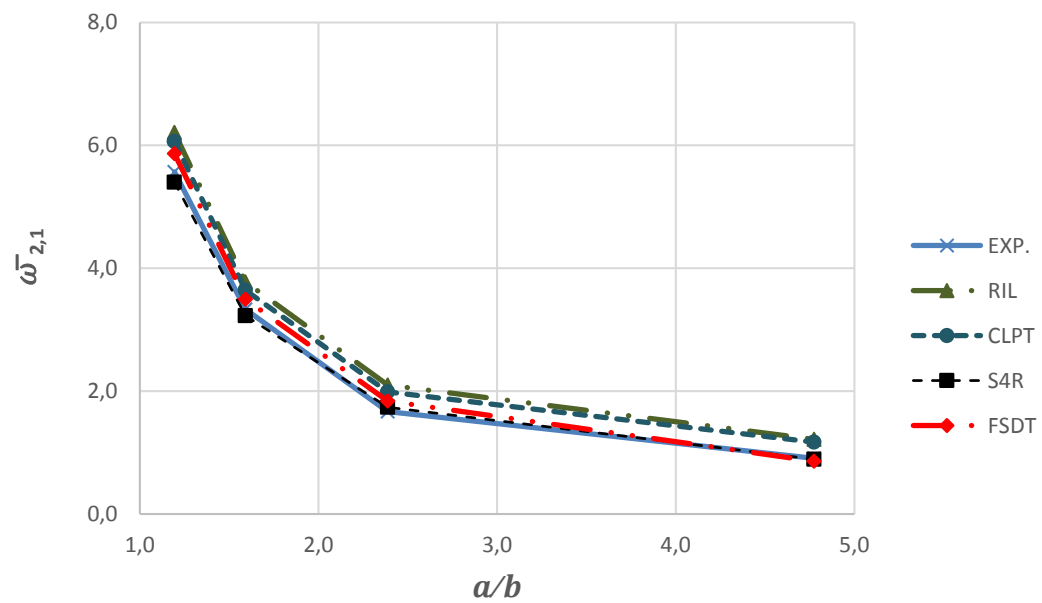
Figure 9. The effect of aspect ratio on nondimensionalized frequencies $\bar{\omega}_{2,1}$.
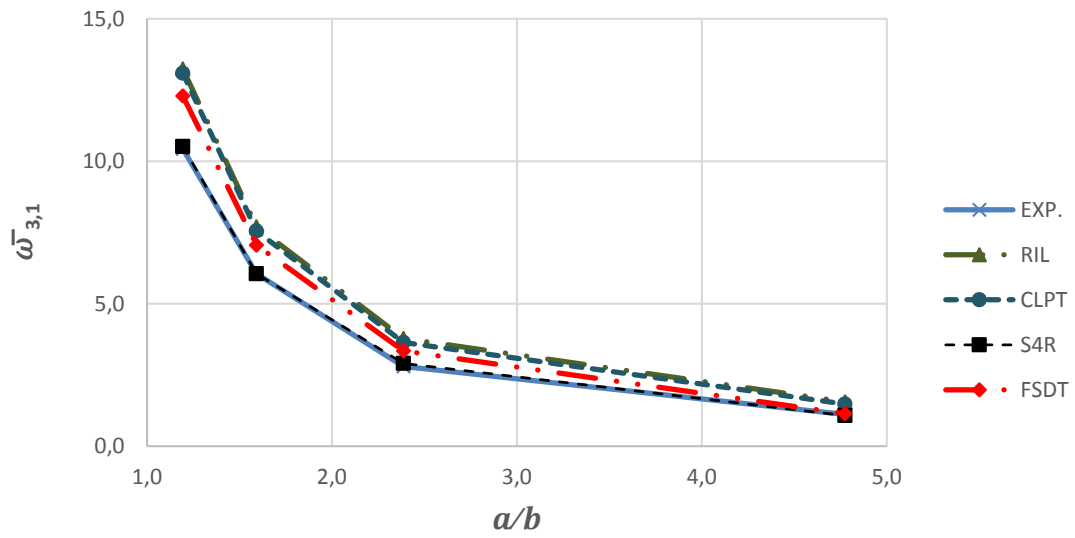
Figure 10. The effect of aspect ratio on nondimensionalized frequencies $\bar{\omega}_{3,1}$.

Table 3. Relative difference in comparison to the mode $f_{m,n}$ (left) and mean difference of the prediction model (right).

Mode $f_{m,n}$	RIL (%)	CLPT (%)	FSDT (%)	S4R (%)		Model	Difference (%)
$f_{1,1}$	38.9	33.6	17.3	19.7		RIL	30.9
$f_{2,1}$	21.3	16.6	6.5	7.4		CLPT	26.2
$f_{3,1}$	32.4	28.3	14.2	2.1		FSDT	12.7
						S4R	9.7

New tests for the CLT plates

Because the exact material properties were not presented in the test carried out by Maldonado & Chui (2012), additional vibration tests with known material properties were conducted in this study. In these experiments, two different rectangular CLT plates were supported on all four sides and the free vibration phenomenon was achieved by impacting the plates with a hammer. Vertical acceleration history of the plates was recorded at three different locations in order to extract modes of vibration in the longitudinal direction. Both the CLT plates had the same in-plane dimensions of 2.45 m x 4.00 m, a density of 470 kg/m^3 and were made of strenght class C24 according to RIL (2009). The first plate, denoted here as CLT 100, was 100 mm thick and consisted of three layers with thicknesses of 30/40/30 mm and a lamination scheme of $90°/0°/90^0$. The lamination scheme represents the orientation of a layer to the longer direction of a plate. The second plate, denoted here as CLT 200, was 200 mm thick and consisted of seven layers with thicknesses of $(20/40/20/40)_{SO}$ mm and a lamination scheme of $(0°/90°/0^0/90°)_{SO}$. In-plane dimensions of the plates and illustrations of the accelerometers are shown in Figure 11.

The vertical acceleration histories were converted into frequency domain by using the fast Fourier transform (FFT) algorithm in order to identify the natural frequencies. For both the CLT 100 and CLT 200 plates, three lowest frequencies, namely $f_{1,1}$, $f_{2,1}$ and $f_{3,1}$, were measured and then compared to the values predicted by the models. The Fourier spectra for the CLT 100 and CLT 200 plates showing the three lowest natural frequencies are shown in Figures 12 and 13, respectively. The measured frequencies and results from the different prediction models as well as the mean errors for the CLT 100 and CLT 200 plates are shown in Tables 4 and 5.

From Figures 12 and 13, the measured frequencies are easily distinguished as peaks in the frequency domain. Similar plots were generated from numerous vibration events and therefore the peaks are considered to genuinely represent the natural frequencies of the plates. It is also noted that for the thinner plate CLT 100 the fundamental frequency is higher despite the fact that it is only half as thick as the CLT 200. This is because its top and bottom layers are parallel to the shorter side of the plate and underlines the importance of adding stiffness in the shorter direction of the plates supported on four sides.

From Table 4 it is noted that all the prediction models produce extremely accurate results (error ~ 5 %) for the CLT 100 plate in comparison with the experimental results. The accuracy of the results is attributed to the relative slenderness (b/h = 25) of the plate which implies that the shear deformation is not significant.

As can be seen from Table 5, the accuracy of the prediction models drops dramatically (error ~ 15-70 %) for the CLT 200 plate even though the lower characteristic values were used for the elastic constants. This is because the side-to-thickness ratio (b/h=12) decreases and the shear deformation becomes significant. On the other hand, it is possible that for the multilayer plate the layers are not perfectly bonded together and result in a lower stiffness than expected. The models that take into account the shear deformation (FSDT and S4R) perform clearly better than the other models (RIL and CLPT). Again, it is noted that the model recommended by the design code (RIL, 2009) should be used with caution with relatively thick CLT plates.
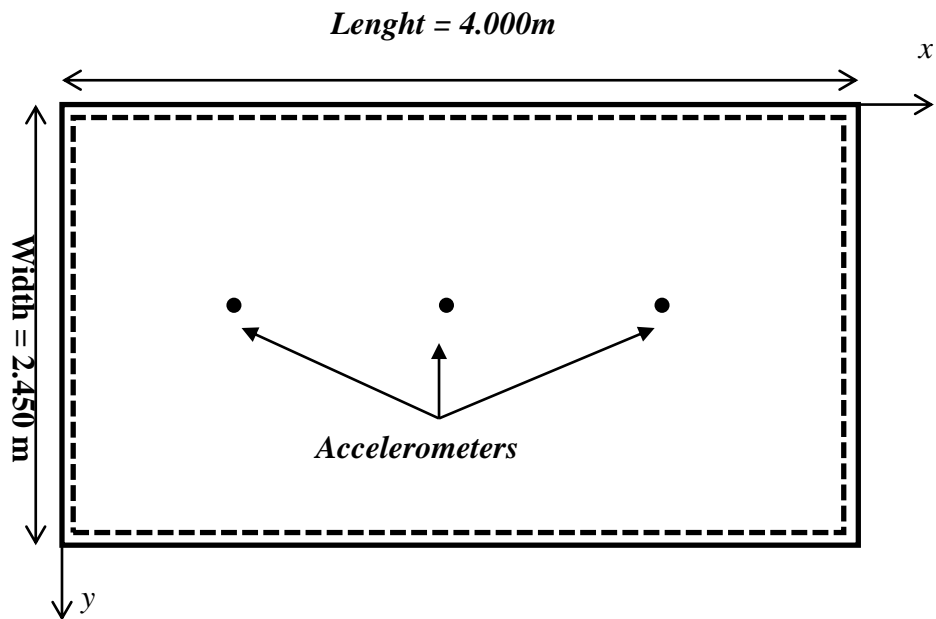
Figure 11. In-plane dimensions and illustration of the accelerometers.
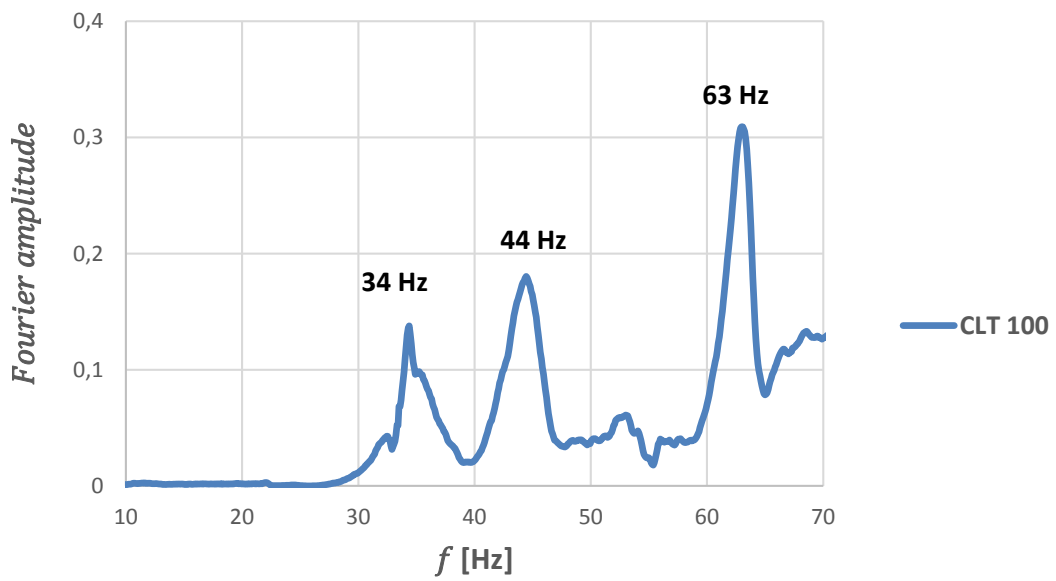
Figure 12. Fourier spectrum for the CLT 100 plate.
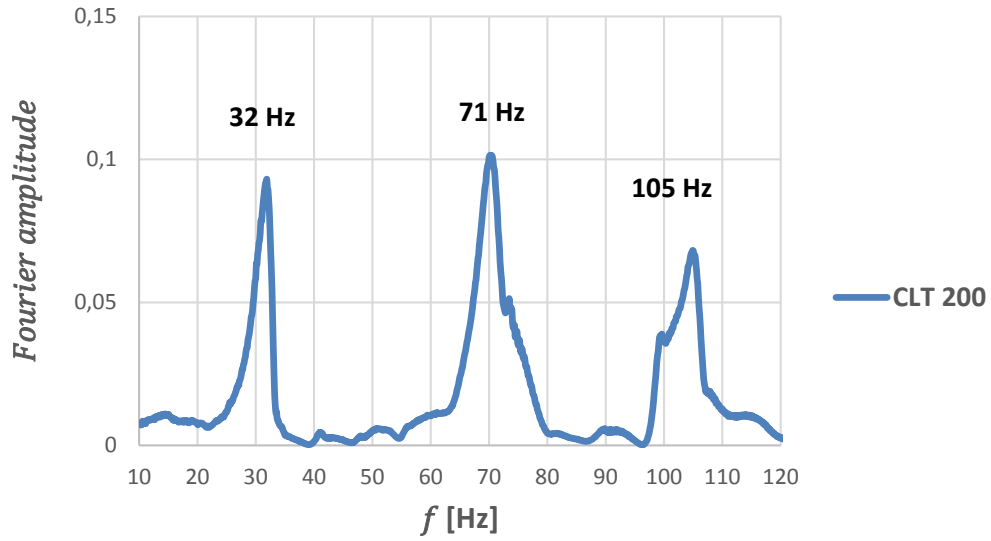
Figure 13. Fourier spectrum for the CLT 200 plate.

Table 4. Experimental values and results from different prediction methods for the CLT 100.

Mode $f_{m,n}$	RIL (Hz)	CLPT (Hz)	FSDT (Hz)	S4R (Hz)	Exp. (Hz)		Model	Difference (%)
$f_{1,1}$	37.1	37.7	36.7	34.1	34.0		RIL	4.9
$f_{2,1}$	44.0	46.0	44.8	41.5	44.0		CLPT	4.5
$f_{3,1}$	59.9	63.2	61.4	58	63		FSDT	3.4
							S4R	5.5

Table 5. Experimental values and results from different prediction methods for the CLT 200.

Mode $f_{m,n}$	RIL (Hz)	CLPT (Hz)	FSDT (Hz)	S4R (Hz)	Exp. (Hz)		Model	Difference (%)
$f_{1,1}$	57.8	49.2	46.5	43.4	32.0		RIL	71.8
$f_{2,1}$	107.8	89	79.2	70.9	71.0		CLPT	46.8
$f_{3,1}$	192.3	169.3	134.2	114.1	105.0		FSDT	28.2
							S4R	15.2

Conclusion

The basic principles concerning the dynamical behavior of a simply supported specially orthotropic plate were explained through various prediction models. Mode shapes of a CLT floor remain aligned with the laminate coordinate system because the stiffness matrix coefficients related to twisting moments disappear with the symmetric laminates with multiple specially orthotropic layers. Natural frequencies increase as the plate aspect ratio (a/b) decreases and the modulus ratio (E_1/E_2) increases. The relative thickness (a/h) has an important effect on the natural frequencies even at moderate values $(a/h = 20)$. Negligence of this leads to overprediction of natural frequencies and in the worst case to serviceability problems with CLT timber floors.

The prediction models were evaluated by comparing them with two laboratory experiments. Since the exact material properties were not known in the first experiment, they were assumed. In the second experiment, two CLT plates with known material properties were tested. Two models (RIL and CLPT) produced results with a notable disagreement with the test results in cases where the shear deformation was significant while the other two models which take into account the shear deformation (FSDT and S4R) agreed quite well with the results. The code based method (RIL) should be used with awareness of its range of applicability for relatively thick CLT floors which tend to be prone to remarkable shear deformation. The shear deformation model FSDT could be a suitable model for vibration analysis for CLT plates but the effect of shear correction factors should be studied in more detail. Finite element model with a shell element which allows shear deformation (S4R) performed in a proper way in every aspect.

In conclusion it can be said that the vibration problem of a CLT plate is a difficult task to formulate in a design code friendly format because of its compliancy to shear deformation. It might also be important to study whether the multilayer CLT plates actually behave in a fully composite manner. However, as illustrated in this study, more refined plate theories or finite element analysis programs can be used to predict the dynamical behavior of CLT structures accurately.

Acknowledgements

References

Abaqus, 2012. *Abaqus Version 6.12 Documentation.* Providence, RI, USA: Dassault Systèmes Simulia Corp.

CEN, 2004. *Eurocode 5: Design of timber structures. Part 1-1: General. Common rules and rules for buildings.* Brussels: European Committee for Standardization.

Gsell, D. et al., 2007. Cross-Laminated Timber Plates: Evaluation and Verification of Homogenized Elastic Properties. *Journal of Structural Engineering,* 133(1), pp. 132-138.

Hamm, P., Richter, A. & Winter, S., 2010. Floor vibrations - new results. In: A. Ceccotti, ed. *11th World Conference on Timber Engineering 2010 (WCTE 2010). Proceedings of a meeting held 20-24 June 2010, Trentino, Italy..* Red Hook, NY, USA: Curran Associates, Inc., pp. 2765-2774.

Hu, L. & Gagnon, S., 2012. Controlling cross-laminated timber (CLT) floor vibrations: fundamental and method. In: P. Quenneville, ed. *World Conference on Timber Engineering 2012 (WCTE 2012). Proceedings of a meeting held 15-19 July 2012, Auckland, New Zealand..* Red Hook, NY, USA: Curran Associates, Inc., pp. 269-275.

Maldonado, S. A. H. & Chui, Y.-H., 2012. Vibrational Performance of Cross Laminated Timber Floors. In: P. Quenneville, ed. *World Conference on Timber Engineering 2012 (WCTE 2012). Proceedings of a meeting held 15-19 July 2012, Auckland, New Zealand..* Red Hook, NY, USA: Curran Associates, Inc., pp. 370-377.

Reddy, J. N., 2003. *Mechanics of laminated composite plates and shells: theory and analysis.* 2 ed. Boca Raton, Florida, USA: CRC Press.

RIL, 2009. *RIL 205-1-2009. Puurakenteiden suunnitteluohje. Eurokoodi EN 1995-1-1.* Helsinki: Suomen Rakennusinsinöörien Liitto RIL ry.

Stürzenbecher, R., Hofstetter, K. & Eberhardsteiner, J., 2010. Structural design of Cross Laminated Timber (CLT) by advanced plate theories. *Composites Science and Technology,* 70(9), pp. 1368-1379.

Jussi-Pekka Matilainen, Jari Puttonen
Aalto University, School of Engineering,
Department of Civil and Structural Engineering
PO Box 12100
FI - 00076 Aalto
jussi-pekka.matilainen@outlook.com, jari.puttonen@aalto.fi